

## The Effect of Environment on the Stability of an Integral Membrane Helix: Molecular Dynamics Simulations of Surfactant Protein C in Chloroform, Methanol and Water

Helena Kovacs<sup>1</sup>, Alan E. Mark<sup>1</sup>, Jan Johansson<sup>2</sup>  
and Wilfred F. van Gunsteren<sup>1\*</sup>

<sup>1</sup>Laboratory of Physical Chemistry, ETH-Zentrum CH-8092 Zürich, Switzerland

<sup>2</sup>Department of Medical Biochemistry and Biophysics Karolinska Institutet S-171 77 Stockholm, Sweden

A series of three molecular dynamics simulations at 300 K in explicit solvent environments of chloroform, methanol and water has been performed on the pulmonary surfactant lipoprotein, SP-C, comprising several consecutive valine residues in order to investigate the stability of the  $\alpha$ -helical conformation. Two additional simulations were performed on truncated SP-C with a five-residue N-terminal deletion at 300 K and 500 K in water, the high temperature run in order to increase the rate of peptide denaturation.

Indications of destabilization appear in chloroform during 1 ns while the SP-C  $\alpha$ -helix is remarkably stable during 1 ns in methanol and water. In particular the polyvalyl part comprising residues Val15 to Val21 remains intact even at elevated temperature, and the valines do not disrupt the  $\alpha$ -helical conformation. The valyl-rotamer sampling is partly restricted. Unfolding takes place successively along the primary sequence starting from the C-terminal end. Factors affecting polypeptide stability in molecular dynamics simulations are addressed. The intrinsic helix-forming tendency of valine residues and its dependence on the sequence context, and the role of the solvent environment in stabilizing or destabilizing an  $\alpha$ -helical fold, are discussed.

**Keywords:**  $\alpha$ -helix stability; peptide conformation; solvent interactions; molecular dynamics; computer simulation

\*Corresponding author

### Introduction

Much attention has been focused on the intrinsic helix-forming properties of individual amino acids and on the stability of single  $\alpha$ -helical peptides in solution. This is not least because the insights thus obtained contribute to our understanding of protein stability and folding. The studies have utilized experimental methods, predominantly circular dichroism (CD) and nuclear magnetic resonance (NMR) spectroscopy, as well as computational approaches

such as molecular dynamics (MD) or Monte Carlo simulations and free energy calculations. The majority of these investigations have concerned water soluble proteins. Thus, an aqueous environment has been inherent in the results. The stability of the  $\alpha$ -helical fold in a non-aqueous environment is likewise of biological relevance. For instance, the  $\alpha$ -helical fold is thought to be the predominant conformational motif of proteins located in the membrane interior. In fact, it has been proposed that individual  $\alpha$ -helices spanning a membrane core are sufficiently stable to form as autonomous folding units, which, in the case of a multi-helix protein, topologically rearrange to achieve the complete protein fold (Popot, 1993). In contrast, soluble  $\alpha$ -helices of comparable length are often only marginally stable in aqueous solution without the cooperative effect of tertiary packing interactions.

There is thus considerable interest in an understanding of the effect of environment on both

Abbreviations used: MeA,  $\alpha$ -methylalanine; Aib, aminoisobutyric acid; BPTI, bovine pancreatic trypsin inhibitor; CD, circular dichroism; DPPC, dipalmitoyl-phosphatidylcholine, DSSP, Defining secondary structure of proteins; MD, molecular dynamics; NMR, nuclear magnetic resonance; RDS, respiratory distress syndrome; r.m.s.d., root mean square deviation; SPC, simple point charge; SP-C, surfactant protein C.

helix forming propensity and helix stability. In all cases the overall stability of a given helix will depend on a subtle energetic balance between interactions between (spatially) neighboring amino acids in the polypeptide chain and interactions to the solvent environment. Stability also depends on the changes in the arrangement of the surrounding medium that the presence of the protein introduces. Experimentally it is not possible to analyze such effects at an atomic level. To obtain a detailed picture of the factors that give rise to helix stability it is necessary to turn to theoretical models and numerical simulations.

One approach to elucidate the factors that govern helix stability is to study model systems that comprise a single helical domain. A particularly intriguing case is that of the lung surfactant protein, SP-C. This protein is an essential component of pulmonary surfactant, a mixture of mainly phospholipids and a few specific proteins which reduces the surface tension at the alveolar air/liquid interface and thereby prevents alveolar collapse at end expiration (see Johansson *et al.*, 1994a; Robertson *et al.*, 1992). As respiratory distress syndrome (RDS) in premature infants is due to lack of pulmonary surfactant, development of pharmacological analogues to its components, especially the hydrophobic proteins, is of interest. The function of SP-C appears to be related to the transitions of the surfactant lipids between multiple, double and monolayer structures, although the molecular mechanisms are not settled.

The feature of SP-C that makes its stability of particular interest is that the native structural motif, an  $\alpha$ -helix, contains stretches of seven and four consecutive valine residues. A structure prediction using the statistical method of Chou & Fasman (1978) suggests that SP-C would form a  $\beta$ -sheet structure. Presumably this is because of the high number of valine residues (13 out of 35 residues) which are under-represented in helices. Experimental studies of conformational preferences of the different amino acids in model peptides (Lyu *et al.*, 1990, 1991; Merutka *et al.*, 1990; O'Neil & DeGrado, 1990; Padmanabhan *et al.*, 1990; Wójcik *et al.*, 1990) also indicate that valine residues have an helix-destabilizing effect in aqueous solutions. The suggested reasons for this are loss of conformational entropy due to side-chain rotamer restriction (Padmanabhan *et al.*, 1990; Lyu *et al.*, 1991) and/or sterical hindrance due to C <sup>$\beta$</sup> -branching with a resulting clash of a methyl group in the  $\gamma$ -position and the carbonyl oxygen in the preceding turn of the helix (O'Neil & DeGrado, 1990). It has been shown that SP-C can fold into either an  $\alpha$ -helix (Pastrana *et al.*, 1991; Vandebussche *et al.*, 1992; Johansson *et al.*, 1994b, 1995a) or dimeric  $\beta$ -sheet structures (Baatz *et al.*, 1992). The structure of SP-C thus raises theoretical questions concerning the intrinsic helix-forming propensity of valine residues and to what extent it depends on the polypeptide sequence or the solvent environment. A series of molecular dynamics simulations has been performed in order to compare the behaviour of the  $\alpha$ -helical fold of SP-C in three different environ-

ments. A high temperature simulation complements the series by yielding one possible unfolding pathway of the polypeptide.

The amino acid sequence of the 4.2 kDa porcine form of SP-C is LRIPCCPVNLKRLVVVVVVVVVVVVVVVVIVGALLMGL (Johansson *et al.*, 1988). The two cysteine residues are stoichiometrically palmitoylated (Curstedt *et al.*, 1990). The NMR structure calculated from distance information based on sequential and medium-range NOE connectivities and  $^3J_{\text{HN}\alpha}$  coupling constants shows that SP-C, in a 1:2 mixture of chloroform and methanol containing 5% 0.1M HCl, is helical between residues 9 and 34 (Johansson *et al.*, 1994b). The eight N-terminal residues and the palmitoyl chains lack a stable regular secondary structure. An NMR secondary structure determination of a peptide comprising the SP-C residues 1 to 17 in dodecylphosphocholine micelles (Johansson *et al.*, 1995a) showed a helical structure between residues 11 and 17, indicating that the structure of native SP-C obtained in organic solvents is valid also in a lipid environment. Furthermore, the  $\alpha$ -helix in native SP-C is about 37 Å long which is nearly identical to the thickness of a dipalmitoylphosphatidylcholine (DPPC) bilayer, making a transmembrane orientation of SP-C in the pulmonary surfactant likely (Johansson *et al.*, 1995a). Such an interpretation is supported by infrared spectroscopy studies on the overall secondary structure content of native SP-C in DPPC/phosphatidylglycerol bilayers, which also indicated that the helical axis is oriented perpendicular to the membrane surface (Pastrana *et al.*, 1991; Vandebussche *et al.*, 1992). Two of the characteristics of SP-C, i.e. the low number of charged and polar residues in the helical middle part and exposure of an extensive lipophilic surface, are typical features of transmembrane helices but the high number of valine residues is unusual.

Several MD-simulations of  $\alpha$ -helical polypeptides in aqueous solution have been reported (DiCapua *et al.*, 1991; Soman *et al.*, 1991; Tirado-Rives & Jorgensen, 1991; Daggett & Levitt, 1992; De Loof *et al.*, 1992; van Buuren & Berendsen, 1993). Except for polyalanine helices (DiCapua *et al.*, 1991; Daggett & Levitt, 1992) the  $\alpha$ -helical starting conformation unfolds within a simulation period of a few hundred picoseconds at room temperature. This is in line with experimental CD and NMR data concerning helicity of these isolated peptide fragments in solution, which indicate that the helical structure is in rapid equilibrium with other conformational states. Tobias & Brooks (1991) have investigated the free energy profile for the helix initiation in alanine and valine pentapeptides by MD simulations. They report that energy minima for the helical and extended conformations are similar in the case of the alanine pentapeptide while for the valine pentapeptide the helical state has a higher energy than a random coil. The free energy coordinate of an  $\alpha$ -helical oligopeptide containing  $\alpha$ -methylalanine (MeA, aminoisobutyric acid, Aib) in vacuum, water and acetonitrile has also been determined (Smythe *et al.*,

**Table 1**Physical properties of the solvents at 298 K<sup>a</sup>

Solvent	Dipole moment (Debye)	Density (g cm <sup>-3</sup> )	Molar volume (cm <sup>3</sup> mol <sup>-1</sup> )	Dielectric constant	Viscosity (cP)	Polarizability ( $\alpha_0/4\pi\epsilon_0$ ) (10 <sup>24</sup> cm <sup>3</sup> )
Chloroform (Dietz <i>et al.</i> , 1984, 1985)	1.04 (gas) 1.10 (MD)	1.480 (exp) 1.484 (MD)	80.7	4.7	0.54	9.5
Methanol (Stouten, 1989)	1.70 (gas) 2.32 (MD)	0.787 (exp) 0.791 (MD)	40.7	32.7	0.54	3.3
Water (Berendsen <i>et al.</i> , 1981)	1.85 (gas) 2.27 (MD)	0.997 (exp) 1.000 (MD)	18.1	78.4	0.89	1.5

<sup>a</sup> Lide (1993).

1993). Helical peptides have also been simulated in pure trifluoroethanol (De Loof *et al.*, 1992) and in 30% trifluoroethanol (van Buuren & Berendsen, 1993). De Loof *et al.* (1992) propose that the well-known helix-stabilizing effect of trifluoroethanol originates from the inability of the large solvent molecules to make hydrogen bonds to the backbone amide protons within the  $\alpha$ -helix. To our knowledge no other equivalent theoretical studies on the stability of  $\alpha$ -helical polypeptides in non-aqueous solvents have appeared. A limited number of other biomolecules has been simulated in pure non-aqueous solvents. These include the globular proteins bovine pancreatic trypsin inhibitor (BPTI) in an apolar atomic solvent (van Gunsteren & Karplus, 1982), BPTI in chloroform (Hartsough & Merz, 1993) and *Rhizomucor miehei* lipase in methyl hexanoate (Norin *et al.*, 1994). Simulations of cyclic peptides in organic solvents include cyclosporin A in carbon tetrachloride (Lautz *et al.*, 1990; El Tayar *et al.*, 1993) and a cyclic hexapeptide in dimethyl sulfoxide (Mierke & Kessler, 1991). None of these solvents can act as a hydrogen-bond donor. The common conclusion from these investigations was that the aprotic organic solvent enhances intramolecular hydrogen bonding. This stabilizes the protein conformation making it more rigid and compact.

As a transmembrane peptide with pronouncedly hydrophobic character, SP-C clearly differs from the previously simulated helical peptides. The molecular dynamics simulations were performed using non-palmitoylated SP-C at 300 K. The simulations were based on the  $\alpha$ -helical SP-C structure. Either chloroform, methanol or water was incorporated as an explicit solvent. In the present study separate simulations in the pure solvents were performed. This is in contrast to the experimental investigation in which an acidified methanol-chloroform mixture was used. The use of pure solvents avoids the difficulty of obtaining a proper equilibration of a mixed solvent within the simulation time span. It also enables a more straight-forward comparison of the solvent-protein interactions.

In previously published MD-simulations it has been shown that water molecules disrupt the helical structure by penetrating into the core of the peptide and replacing hydrogen bonds between the backbone carbonyls and amide protons (DiCapua *et al.*, 1991; Tirado-Rives & Jorgensen, 1991; De Loof

*et al.*, 1992). The solvent molecule's size, polarity and hydrogen-bonding ability affect the interaction of solvent molecules with the protein backbone. The three solvents used in the current study represent a series of solution environments with widely different properties, as illustrated by Table 1. Water is a polar and strongly hydrogen-bonding solvent. Methanol is less polar than water but also a hydrogen-bond donor and acceptor. Chloroform is only slightly polar and aprotic. The simulation in chloroform will, however, more closely model the behavior of the main part of the protein within its biological environment of the hydrophobic interior of a phospholipid bilayer.

## Results

### r.m.s. deviations from the starting structure

Figure 1 shows the root-mean-square deviation (r.m.s.d.) between the starting coordinates and averaged coordinates from successive 15 ps intervals from the trajectory. Only the C $\alpha$  atoms of the helical residues Asn9 to Val28 were included in the

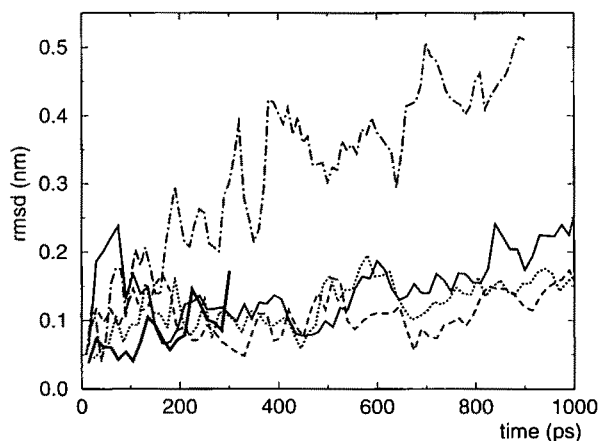


**Figure 1.** Positional root-mean-square difference between the starting coordinates and averaged coordinates obtained from 15 ps subtrajectories. Superposition of the backbone C $\alpha$  atoms of the helical residues Asn9 to Val28 was used both in the subtrajectory averaging and r.m.s.d calculation. SP-C at 300 K in different solvents: solid line, chloroform; broken line, methanol; thick solid line, water; truncated SP-C in water at two temperatures: dotted line, 300 K; dash-dotted line, 500 K.

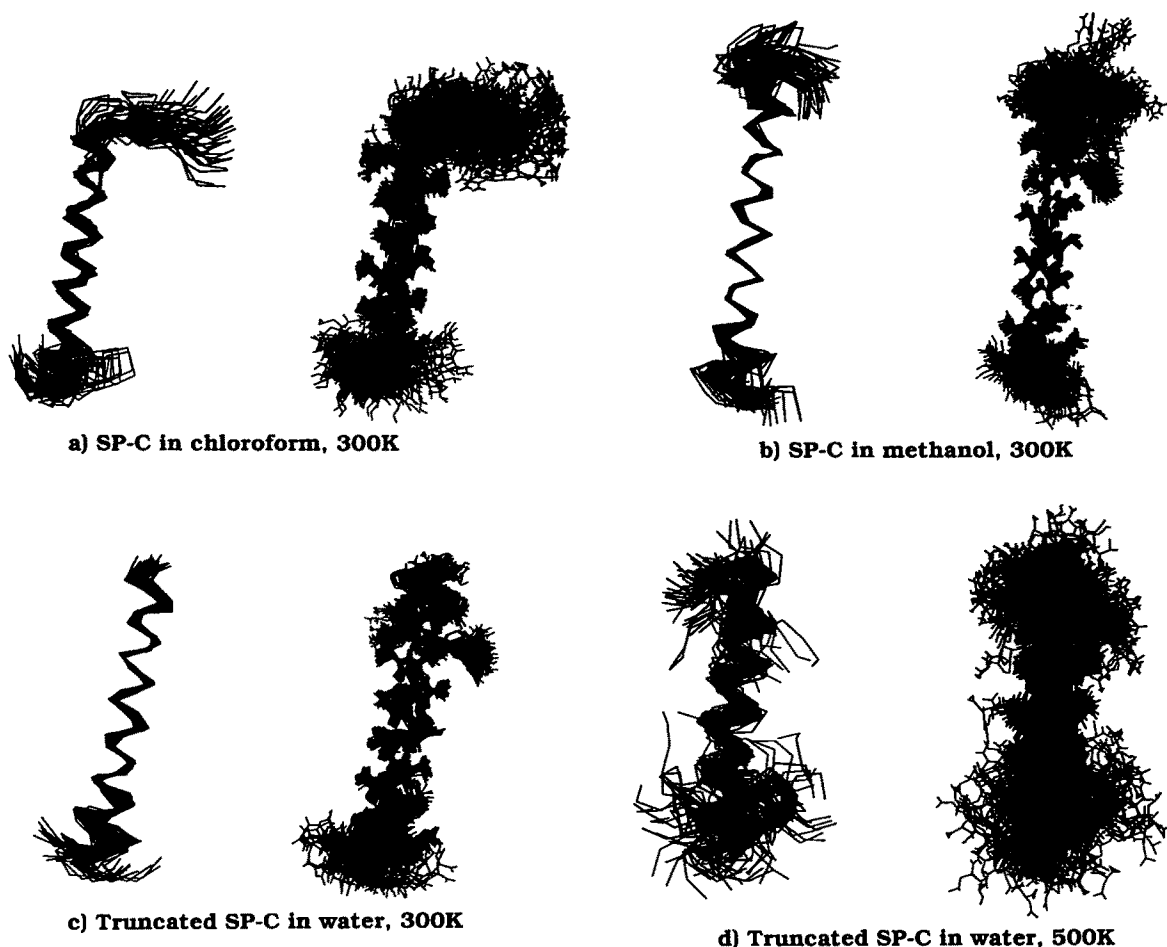


**Figure 2.** Superposition of averaged coordinates from 15 ps consecutive intervals from the trajectories, backbone C $\alpha$  atoms (left) and all atoms (right) are displayed. Only C $\alpha$  atoms of residues Asn9 to Val28 were included in the superposition. The molecules are depicted with the N terminus up and C terminus down. (a) SP-C in chloroform at 300 K, 1.0 ns. (b) SP-C in methanol at 300 K, 1.0 ns. (c) Truncated SP-C in water at 300 K, 1.0 ns. (d) Truncated SP-C in water at 500 K, 0.9 ns.

superpositions to obtain the mean coordinates and when calculating the displayed r.m.s.d. values. Short-time (15 ps) averaging of the coordinates was performed to remove effects due to rapid local fluctuations. The gently rising r.m.s.d. curves indicate a slow destabilization of the SP-C  $\alpha$ -helix. In chloroform the r.m.s.d. curve reaches a final value of  $\sim 2.5$  Å within 1 ns. The rate of increase in r.m.s.d. is slower in methanol reaching a value of  $\sim 1.5$  Å during 1 ns of simulation. The short length of the simulation of the complete SP-C in water, 0.3 ns, impedes comparisons with the longer runs in the organic solvents. The corresponding r.m.s.d. curves for the truncated SP-C in water at 300 K and 500 K are also shown in Figure 1. The r.m.s.d. of the truncated SP-C at 300 K is similar to the r.m.s.d. of the complete peptide both in water and in methanol. The unstructured N-terminal residues do not contribute to the reported r.m.s.d. values and the N-terminal five-residue deletion apparently does not significantly affect the helix-stability. Thus, in the subsequent analysis the 1 ns trajectory of the truncated polypeptide at 300 K is taken to represent the behaviour of SP-C in water. The rapid rise of the

r.m.s.d. curve at 500 K indicates loss of helical conformation at this temperature. Averaged coordinates from each 15 ps interval between 60 to 1020 ps for SP-C in chloroform and methanol are presented in Figure 2(a) and (b), respectively, after a superposition of the C $\alpha$  atoms of residues Asn9 to Val28. Figure 2(c) and (d), respectively, display the averaged coordinates from 15 ps intervals of the truncated SP-C in water at 300 K between 50 to 1010 ps and from 10 ps intervals at 500 K between 10 to 900 ps. The average value of the pairwise r.m.s. deviations of the backbone C $\alpha$  atoms and of all atoms (Figure 2) to their mean, after a superposition of C $\alpha$  atoms in residues Asn9 to Val28, is given in Table 2.

### Backbone and side-chain dihedral angles

Figure 3 displays the Ramachandran plots for the  $\phi$ - $\psi$  backbone dihedral angle pairs in residues Pro7 to Val28, extracted every 3 ps from the 1 ns trajectories in the three solvents and the elevated temperature run. This particular residue interval was chosen because its  $\phi$ - $\psi$  pairs in the methanol

**Table 2**

Root-mean-square positional fluctuations for the backbone C $\alpha$  atoms of residues Asn9 to Val28 and for all atoms within the bundles of coordinates displayed in Figure 2. Superposition of the backbone C $\alpha$  atoms of residues Asn9 to Val28 to the mean coordinates of the bundle

Molecule	Solvent	Temperature (K)	Time (ns)	r.m.s.d. backbone C $\alpha$ (Å)	r.m.s.d. all atoms (Å)
SP-C	Chloroform	300	1.02	1.26	2.90
SP-C	Methanol	300	1.02	0.88	2.36
SP-C	Water	300	0.30	0.69	1.41
Trunc. SP-C	Water	300	1.03	0.85	1.95
Trunc. SP-C	Water	500	0.90	2.25	4.20

simulation (Figure 3(b)) are strictly confined to the  $\alpha$ -helical region with the midpoint of the cluster corresponding to the canonical  $\alpha$ -helix values of  $\phi = -57^\circ$  and  $\psi = -47^\circ$ . There is no indication of strain in the peptide backbone forcing the torsion angles  $\phi$  and  $\psi$  to adopt other than optimal geometry.

The dispersion from the  $\alpha$ -helical region observed in the chloroform trajectory (Figure 3(a)) is caused by the C-terminal fraying of SP-C that affects Val25 to Val28 and a destabilization that affects Val15–Val16 in the middle of the helix. At the elevated temperature (Figure 3(d)) some scattering of the dihedral angle

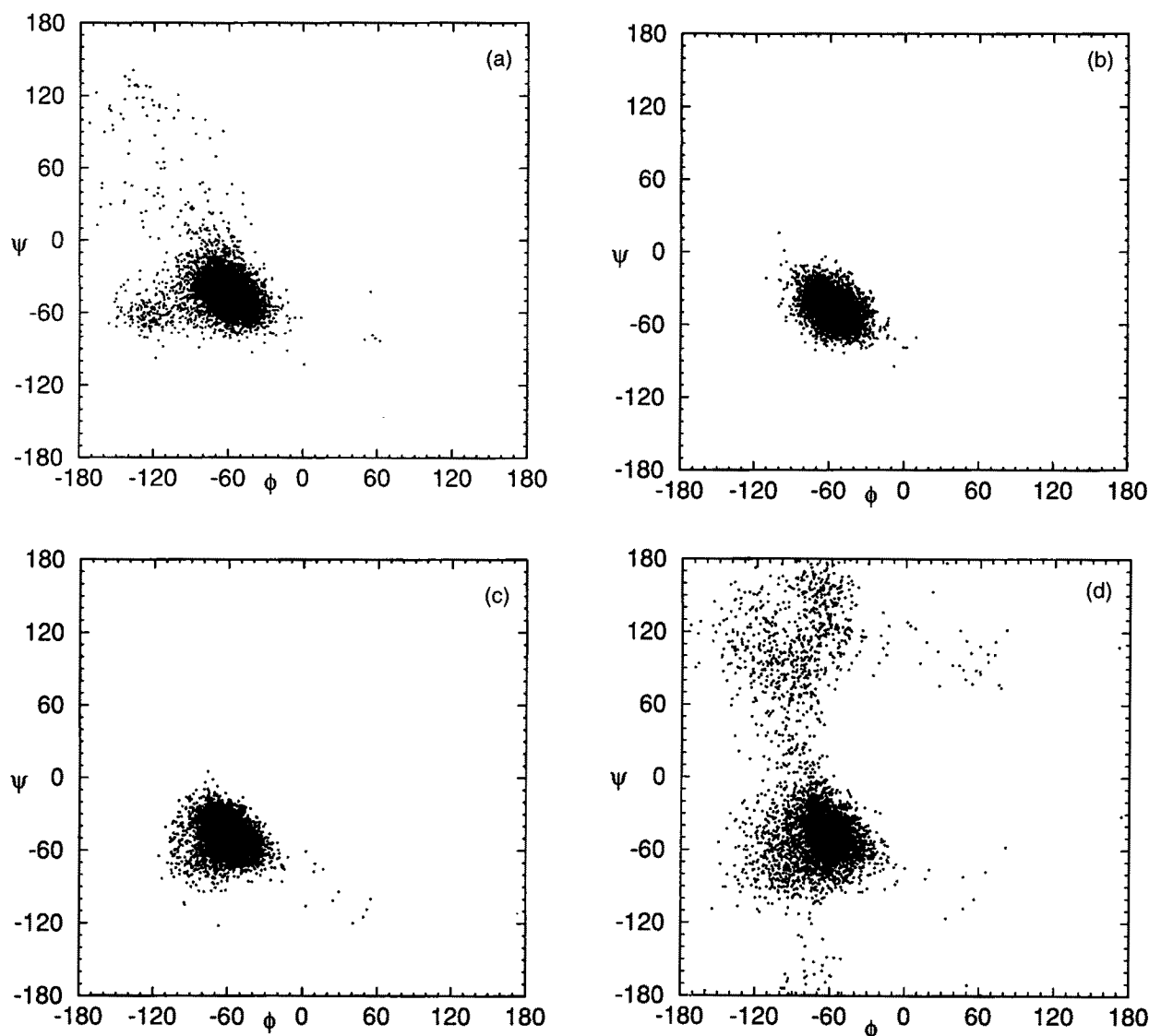


**Figure 3.** Ramachandran plots showing  $\phi$  and  $\psi$  dihedral angle pairs (in degrees) of residues Pro7 to Val28 every 3 ps. (a) SP-C in chloroform at 300 K, 1.0 ns. (b) SP-C in methanol at 300 K, 1.0 ns. (c) Truncated SP-C in water at 300 K, 1.0 ns. (d) Truncated SP-C in water at 500 K, 0.9 ns.

pairs towards the  $\beta$ -region takes place while the majority remains in the  $\alpha$ -helical region.

It has been proposed that the destabilizing effect of valine residues on an  $\alpha$ -helix results from a reduction of configurational entropy associated with the loss of rotational freedom of the valyl side-chains because of packing restrictions (Padmanabhan *et al.*, 1990; Lyu *et al.*, 1991). This hypothesis has been the subject of computational modeling in which the valyl side-chain rotation was investigated in polyalanine environments (Yun & Hermans, 1991; Creamer & Rose, 1992). Averaged over all residues the distribution of valyl side-chain  $\chi^1$ -dihedral angles in the simulated trajectories is similar for the 1 ns simulations in chloroform and methanol. The  $\chi^1$  torsion angles including those within the polyvalyl part (Val15 to Val21) fall close to the optimal rotamer values of  $-60^\circ$ ,  $+60^\circ$  and  $+180^\circ$ . The maximum for the dominant rotamer is slightly shifted to a value of  $-65^\circ \pm 5^\circ$ . The  $+180^\circ$  conformation is noticeably populated only in two cases, Val8 and Val15 in the chloroform simulation. Good packing of valine side-chains in the helical conformation is indicated. There is no indication of conformational strain in the helical segment containing consecutive valine residues due to steric clashes, such as overlap of the bulky  $C^\beta$ -branched residues. It is also worth noting that at room temperature the leucine  $\chi^1$  dihedral angles do not assess the rotamer value of  $+60^\circ$  in any of the simulated trajectories. The absence of this rotamer has been shown by model peptide studies (Lyu *et al.*, 1991) and statistical analyses of protein structures (McGregor *et al.*, 1987; Blaber *et al.*, 1994) to be characteristic for long side-chains inserted into  $\alpha$ -helices. The reason is a steric clash of  $C^\gamma$  in position  $i$  and the carbonyl group in position  $i-3$ .

Another measure of the side-chain rotational freedom is the number of transitions between the three rotamer energy minima. The number of  $\chi^1$ -transitions per valine residue during 1 ns is 3.7 in chloroform, whereas only 2.0 in methanol. For comparison, the corresponding number of  $\chi^1$  transitions per leucine residue is considerably higher, that is, 8.6 in chloroform and 11.0 in methanol. The  $\chi^2$  transitions per leucine residue are 22.1 in chloroform and 22.2 in methanol, implying free rotation. The comparatively low number of  $\chi^1$  transitions in valine shows that there is some, although not complete, rotamer restriction. In chloroform the conformational freedom of the valine side-chains is larger than in methanol. A number of valine residues show no  $\chi^1$  transitions during the simulation period, for example, Val21 in chloroform and Val8, Val20, Val21 and Val23 in methanol. This suggests that the restriction of the side-chain rotamer sampling is position dependent. The length of the simulation and the total number of transitions is, however, insufficient for a statistically valid analysis of the  $\chi^1$  distributions of the individual valine residues.

## Inter- and intramolecular hydrogen bonds

The destabilization of the SP-C  $\alpha$ -helix during the simulations is illustrated in Figure 4 where the predominant hydrogen bonds between an amide proton of residue  $i$  and the carbonyl in position  $i-4$  in the SP-C backbone are displayed. The criteria used to define a hydrogen-bonding interaction were that the hydrogen-acceptor distance was less than 2.5 Å and the donor-hydrogen-acceptor angle was larger than  $135^\circ$ . Hydrogen bonds with an average occupancy of 50% or more for successive 60 ps intervals are displayed. The  $(i, i-4)$  hydrogen bond is a sensitive indicator of  $\alpha$ -helical conformation. However, the backbone angles may reside close to the optimal helical values without the amide-hydrogen atom in position  $i$  and the carbonyl-oxygen atom of residue  $i-4$  being within a hydrogen-bonding distance (Daggett & Levitt, 1992). At the outset of the simulations the regular  $\alpha$ -helical hydrogen bonds were present in the segment Cys6 to Gly34 of the complete SP-C and in the segment Pro7 to Gly34 of the truncated protein.

In chloroform the characteristic hydrogen bonds in the polyvalyl region remain reasonably intact throughout the simulation (compare Figure 4(a)). The C-terminal fraying of the  $\alpha$ -helix begins immediately and progresses successively up to the position of Val20 during 1 ns. The regular  $\alpha$ -helical hydrogen-bonds are replaced in chloroform mainly by  $\text{NH}_i-\text{CO}_{i-3}$  hydrogen bonds. It has been previously observed in MD-simulations that the unfolding of an  $\alpha$ -helix proceeds *via* a  $3_{10}$ -helix (Soman *et al.*, 1991; Tirado-Rives & Jørgensen, 1991; De Loof *et al.*, 1992). It is, however, possible that the predominance of this mechanism is an artifact of the nature of the force field used. Fluctuations between an  $(i, i-4)$  and  $(i, i-3)$  hydrogen-bond, that is, between an  $\alpha$  and  $3_{10}$ -helical conformation, were observed around Arg12 and particularly at Val15 in chloroform. This instability does not, however, lead to unfolding. These fluctuations are a consequence of intramolecular polar interactions between the backbone carbonyl groups and the charged side-chains Arg2, Lys11 and Arg12 rather than interactions with the solvent. Most of the time, however, the polar and charged groups in the side-chains and termini find other hydrogen-bonding partners than the backbone atoms participating in  $\alpha$ -helical hydrogen bonds. Due to these rearrangements of charged side-chains and termini, the electrostatic energy of the protein in chloroform goes down from  $+0.51$  to  $-0.45$  kJ mol $^{-1}$  during 1 ns. This is in contrast to the intramolecular van der Waals energy of the protein which remains essentially constant throughout the simulation. The intramolecular Coulomb and van der Waals energies of the protein simulated in methanol and in water at room temperature, also remain virtually constant throughout the simulations. At elevated temperature the van der Waals contribution remains constant but around 800 ps of simulation the electrostatic protein-protein energy drops from  $-0.09$  to  $-0.41$  kJ mol $^{-1}$ . The

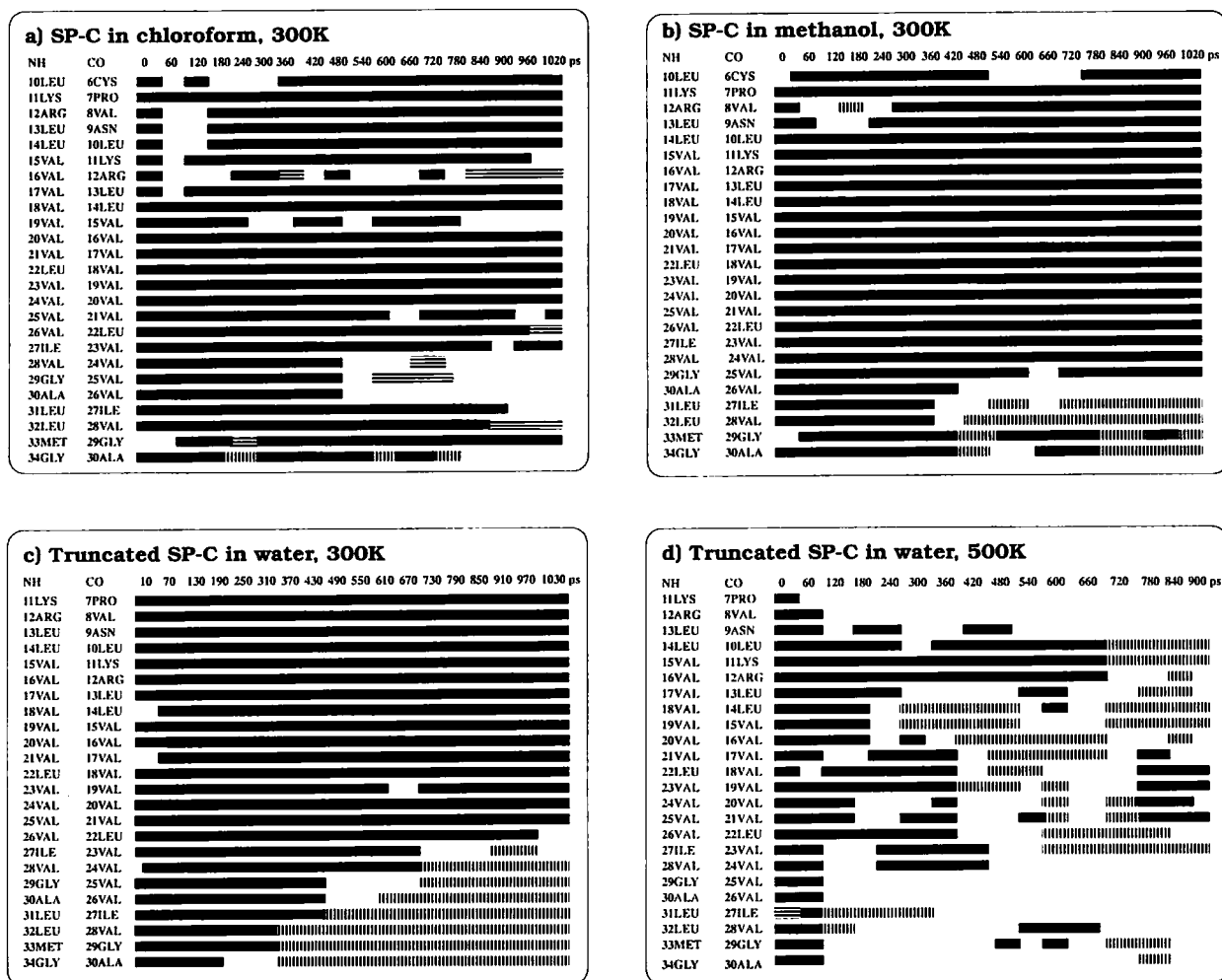


**Figure 4.** Presence of backbone  $\text{NH}_i\text{-CO}_{i-4}$  hydrogen bonds found in 60 ps subtrajectories. The  $(i, i-4)$  hydrogen bonds with occupancy higher than 50% are denoted with a solid bar. A horizontally striped bar denotes  $(i, i-3)$  hydrogen bonds and vertically striped bar denotes  $(i, i-5)$  hydrogen bonds, both with an occupancy higher than 50%. (a) SP-C in chloroform at 300 K, 1.0 ns. (b) SP-C in methanol at 300 K, 1.0 ns. (c) Truncated SP-C in water at 300 K, 1.0 ns. (d) Truncated SP-C in water at 500 K, 0.9 ns.

displacement of the C terminus to within a close distance to the positively charged residues in the N terminus causes this energy drop.

In methanol the residues Asn9 to Val28 retain the canonical  $\alpha$ -helical conformation (Figure 3(b)) and their  $\alpha$ -helical hydrogen bonds remain intact (compare Figure 4(b)). The charged side-chains and termini do not disrupt the  $\alpha$ -helix by forming intramolecular hydrogen bonds to the protein backbone in methanol as they do in chloroform. That is because they are solvated. At 360 ps in the methanol simulation there is a cooperative transition involving the C-terminal residues Ala30 to Gly34. The  $\alpha$ -helical hydrogen bonds are replaced by  $(i, i-5)$  hydrogen bonds resulting in a conformation that is essentially retained throughout the rest of the simulation in spite of some fluctuations. This conformation was identified by the DSSP (Defining Secondary Structure of Proteins) algorithm of Kabsch & Sander (1983) as  $\pi$ -helix.

Table 3 lists the percentage of intermolecular

hydrogen-bonding interactions between the protein and polar solvents. The interactions of the solvent molecules with the polypeptide backbone are fewer in methanol than in water. Within the polyvalyl part, in particular, methanol does not interact with the backbone at all, while water does so to some extent. One of the first residues to lose the  $(i, i-4)$  hydrogen bond is Ala30 as seen in Figure 4(a) to (d). At this position the polar solvent molecules have access to the polypeptide backbone and form intermolecular hydrogen bonds to the carbonyl oxygen atom and the amide hydrogen atom of Ala30 (Table 3). A possible explanation is conformational flexibility and steric effects at this site due to the proximity of Gly29. In chloroform where the solvent hardly can compete for polar interactions, the C-terminal carboxy-oxygen atoms, instead, make polar contacts with the Ala30 backbone amide proton and also with Val28 and Gly29 backbone amide hydrogen atoms during the last 100 ps of the simulation.

The results for the complete SP-C during the 300 ps of simulation in water are fairly similar to the methanol data within the same time period. The  $(i, i - 4)$  hydrogen bonds remain practically intact along the whole length of the  $\alpha$ -helix. The only intramolecular side-chain interaction observed is a polar bridge between the Arg12 side-chain and the Asn9 side-chain. The occupancy of  $\alpha$ -helical hydrogen bonds in the truncated SP-C in water at 300 K and 500 K are shown in Figure 4(c) and (d), respectively. At 300 K the overall behaviour of the  $\alpha$ -helix is similar to that in methanol. The truncated N terminus remains completely intact and there is a gradual opening up of the C terminus into a  $\pi$ -helical conformation. Around 310 ps at 300 K the C-terminal residues Leu32 to Gly34 simultaneously exhibit a transition from  $(i, i - 4)$  to  $(i, i - 5)$  hydrogen bonds. In water the  $\pi$ -helix structure becomes extensive involving eight residues, Val27 to Gly34, and it is stable throughout the simulation. Such a secondary structure element is rarely found in native proteins in aqueous solutions (Kabsch & Sander, 1983). This is because it presumes a cavity in the middle of the helix and somewhat unfavorable backbone torsion

angles,  $\phi = -57^\circ$  and  $\psi = -70^\circ$  (Creighton, 1984). The midpoint of the cluster of the  $\phi$ - $\psi$  pairs for residues Val28 to Met33 during the last 300 ps of the water simulation is located at  $\phi = -60^\circ$  and  $\psi = -65^\circ$ . At the elevated temperature of 500 K in water the  $\alpha$ -helical hydrogen bonds rapidly interchange with  $(i, i - 3)$  and  $(i, i - 5)$  hydrogen bonds. The backbone hydration increases at the elevated temperature according to the intermolecular hydrogen-bond data of Table 3. Nevertheless, even at 500 K a close approach of the solvent to the backbone amide protons is prevented within the polyvalyl segment of Val15 to Val21.

### Surface areas

It is expected that in polar solvents, particularly water, proteins seek to expose backbone polar groups to the solvent and at the same time to bury aliphatic hydrophobic side-chains. In a less polar solvent, such as chloroform, it might be expected that the opposite would happen, i.e. the exposed hydrophobic surface area would increase. To detect such tendencies in the current system the solvent

**Table 3**

Occupancy (in %) of intermolecular hydrogen bonds in the simulated trajectories

	Main-chain CO as acceptor			Main-chain NH as donor		
	SP-C in methanol 300 K	Trunc. SP-C in water 300 K	500 K	SP-C in methanol 300 K	Trunc. SP-C in water 300 K	500 K
Leu1	3					
Arg2	8			5		
Ile3						
Pro4	1					
Cys5	4			85		
Cys6		1	34	31		
Pro7		8	44			
Val8		15	54	6	63	52
Asn9		12	10		14	53
Leu10		17	11	2		46
Lys11		3	16		1	53
Arg12		7	12			16
Leu13		8	4			5
Leu14		9	10			2
Val15		5	26			1
Val16		7	25			
Val17		3	25			
Val18		8	13			
Val19		29	14			
Val20		19	28			
Val21		14	14			
Leu22		9	10			1
Val23		5	29		1	2
Val24		13	47			5
Val25		43	54			3
Val26		12	44			1
Ile27		15	32			
Val28	5	4	27			8
Gly29		8	22		1	25
Ala30	1	62	60	5	6	49
Leu31	13	84	75		1	21
Leu32	8	99	71			2
Met33	9	101	77			7
Gly34	5	103	84			32
Leu35				6	25	36

A value higher than 100% indicates multiple hydrogen bonds. Empty reading signifies 0%.

**Table 4**

Absolute sum over solvent exposed surface (in nm<sup>2</sup>) in the starting and final conformations

	All atoms	Non-polar side-chain	Polar side-chain	Total side-chain	Main-chain
SP-C in chloroform (probe radius 0.23 nm)					
Start	34	30	2	32	2
Final	40	34	3	37	3
SP-C in methanol (probe radius 0.17 nm)					
Start	32	28	2	30	2
Final	36	29	4	33	3
Truncated SP-C in water (probe radius 0.14 nm)					
Start	29	25	2	27	2
Final, 300 K	27	23	2	25	2
Final, 500 K	25	19	2	21	4

accessible areas of the starting and final conformations of the simulated polypeptide, were analyzed (compare Table 4). Calculation of solvent accessible surface area (Hubbard & Thornton, 1993) is based on rolling a probe of a given size around a van der Waals surface. Since chloroform, methanol and water differ significantly in size, different estimates of probe radius were used for the three solvents. The same trends in the results were, however, observed when a probe radius appropriate for water was used in all cases. It should be noted that the starting conformations of the full-length and truncated SP-C used in the simulations differ in the respect that the former was extensively optimized in vacuum while the latter was an unoptimized modeled structure. This difference is reflected in Table 4, where the total solvent accessible surface of the full-length SP-C increases both in chloroform and methanol, whereas it decreases in water for the truncated polypeptide. The GROMOS vacuum force field is purely attractive at long range. Vacuum boundary conditions also resemble an extremely hydrophobic environment (Shi *et al.*, 1988). These two factors combine to account for the lower overall accessible surface area of the optimized structure.

The effect of the different solvents becomes, however, evident when the change in polar and non-polar surface area is compared. The increase in total surface area in chloroform is predominantly due to a growing exposure of non-polar side-chains whereas in methanol both the polar and non-polar side-chains become exposed. In water the decrease is due to burial of the aliphatic side-chains. In all cases the increase in the backbone exposure is similar. Overall the changes in solvent accessible surface area are qualitatively as expected, but of minor size.

An analysis of the solvent accessible surface areas for residues Val28 to Met33 in the starting and final conformations renders a plausible explanation to the C-terminal transition from  $\alpha$  to  $\pi$ -helix observed in the methanol and water simulations at room temperature. Such a conformational transition brings about concomitantly a reduction in the exposed hydrophobic surface of the side-chains and a gain in the exposure of the polar main-chain groups. It cannot be excluded, however, that the effect is an artifact due to the force field used.

### Comparison with NMR data

In order to compare the results from the simulations to the experimental NMR data (Johansson *et al.*, 1994b) averaged values for the  $^3J_{\text{HN}\alpha}$  coupling constants were extracted from the simulated trajectories of the full-length SP-C in chloroform, methanol and water using the Karplus equation (Pardi *et al.*, 1984). They are presented in Figure 5 together with the measured values. The overall agreement between the calculated and experimental  $^3J_{\text{HN}\alpha}$  coupling constants is good but some differences appear in chloroform and in the C-terminal region. In all of the five simulations presented here fraying of the  $\alpha$ -helix starts from the C terminus. A similar observation has been reported by Soman *et al.* (1991) and De Loof *et al.* (1992). In the case of SP-C, however, the NMR data clearly indicates that the native structure adopts a regular helical conformation up to Gly34, as confirmed

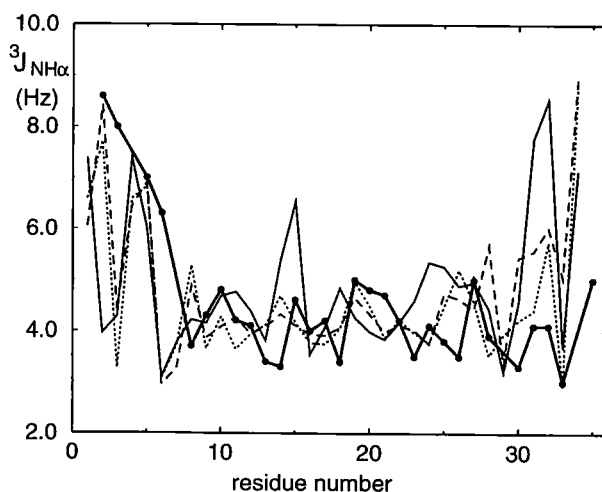


**Figure 5.** Averaged  $^3J_{\text{HN}\alpha}$ -coupling constants for each residue in full-length SP-C extracted from the 60 to 1020 ps trajectories in chloroform and methanol, and from the 60 to 300 ps trajectory in water. The experimental values are taken from the NMR study of Johansson *et al.* (1994b) in a mixed solvent of chloroform, methanol and 0.1 M HCl. Solid line, chloroform; broken line, methanol; dotted line, water; solid thick line with filled circles, NMR data.

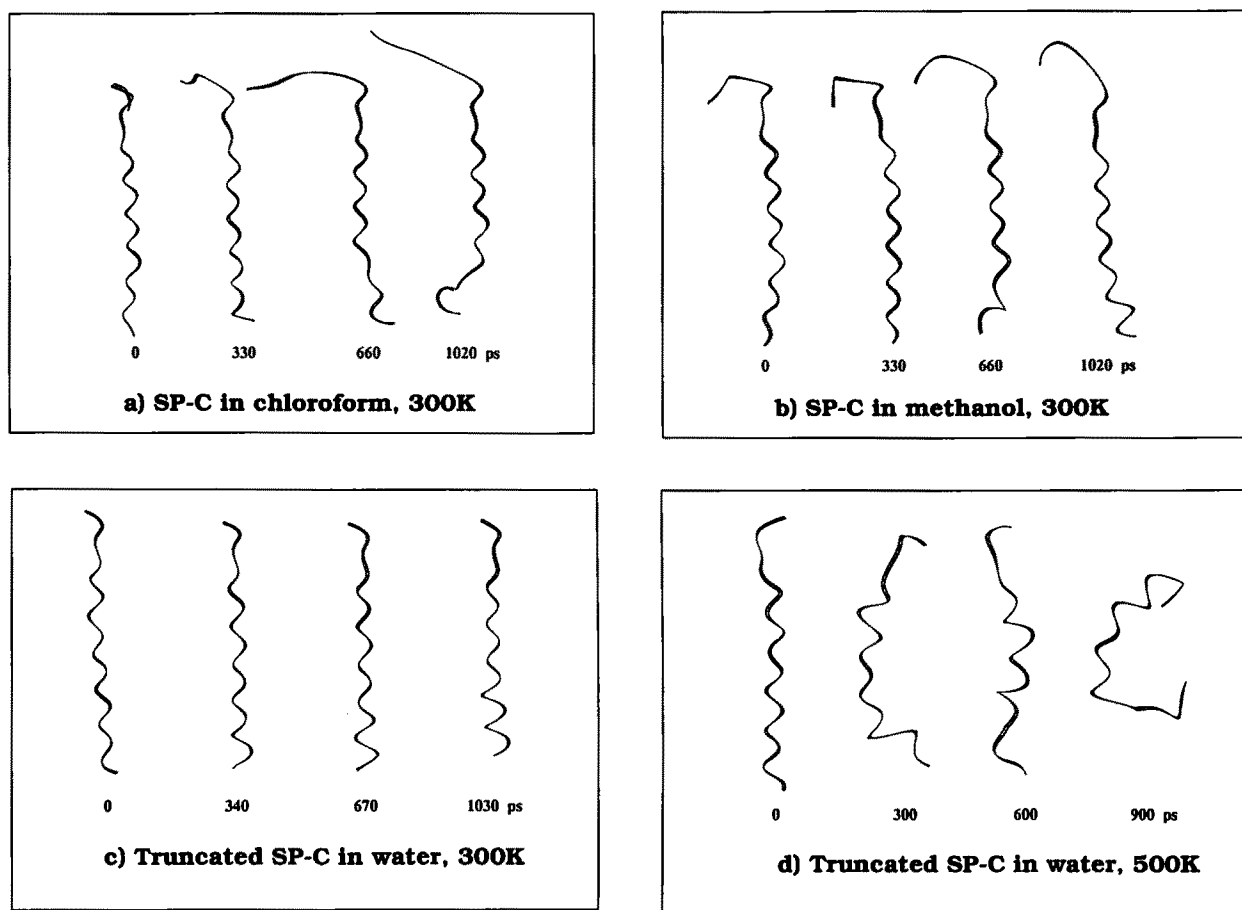


**Figure 6.** Snapshots of the SP-C backbone at successive time points showing the fraying of the helix. The molecules are depicted with the N terminus up and C terminus down. (a) SP-C in chloroform at 300 K, 1.0 ns. (b) SP-C in methanol at 300 K, 1.0 ns. (c) Truncated SP-C in water at 300 K, 1.0 ns. (d) Truncated SP-C in water at 500 K, 0.9 ns.

particularly by the presence of characteristically low  $^3J_{\text{HN}\alpha}$  coupling values. In contrast, in the chloroform simulation the C terminus opens up completely giving rise to intermediate values for the  $^3J_{\text{HN}\alpha}$  coupling constants from position 30 to 35. In the methanol simulation the C terminus adopts the  $\pi$ -helix type of conformation accompanied with partial averaging out of the  $^3J_{\text{HN}\alpha}$  coupling values. The agreement between the NMR data with the water simulation data is better, but one should keep in mind that it is based on only 300 ps of the full-length SP-C simulation, in which the conformational changes were minor.

A total of 244 NOE-based distance bounds used in the NMR structure determination (Johansson *et al.*, 1994b) were compared with the average distances from the trajectories of full-length SP-C. The number of violations using  $\langle 1/r^3 \rangle$  averaging (Tropp, 1980) larger than 0.5 Å was 21 in the chloroform trajectory, 15 in methanol and 12 in water. The majority of the violations occurred in the C-terminal part comprising residues Val26 to Leu35, implying that the NOE-derived conformational space in the mixed solvent does not accommodate the C-terminal unfolding that takes place in the pure solvent simulations. The clear discrepancy between the

NMR data and the results from the simulations in the C-terminal regions can be attributed to the fact that experimental data were obtained in 5% 0.1 M HCl. In this case the carboxy terminus is protonated and thus neutral. In the simulations the C terminus was negatively charged. In chloroform this led to destabilization of the C terminus by direct interaction of the carboxyl group with the amide protons of Val28, Gly29 and Ala30. In methanol and water no direct interaction of the charged C terminus with the polypeptide backbone was observed.

## Discussion

The most dramatic feature of the present MD-study is that the  $\alpha$ -helical conformation of SP-C remains stable during the course of the 1 ns simulations at 300 K. No precautions were taken against possible destabilizing factors such as removal of the C-terminal charge, and non-palmitoylated SP-C, which has a lower  $\alpha$ -helical content than palmitoylated SP-C (Vandenbussche *et al.*, 1992), was simulated. Figure 6 displays snapshots of the polypeptide backbone during the course of the simulations. The C-terminal fraying of the polypeptide helix in chloroform is illustrated, as is the

**Table 5**

Characterization of the simulated systems. The reported energies are an average over the last 60 ps of simulation

	Number of atoms	Temperature (K)	Initial box volume (nm <sup>3</sup> )	Length of simulation (ns)	Protein-solvent energy van der Waals (10 <sup>3</sup> kJ mol <sup>-1</sup> )	electrostatic (10 <sup>3</sup> kJ mol <sup>-1</sup> )
Chloroform	9935	300	261	1.02	-1.73	-0.57
Methanol	11362	300	261	1.02	-0.91	-3.47
Water	19966	300	200	0.30	-0.64	-3.89
Truncated SP-C in water						
300 K	5624	300	60 <sup>a</sup>	1.03	-0.53	-2.97
500 K	11462	500	116	0.90	-0.45	-2.46

<sup>a</sup> A rectangular box was used instead of the truncated octahedron used in the other simulations.

stability of the  $\alpha$ -helix in methanol. The impression that the C terminus of the truncated SP-C helix becomes shorter in water at 300 K (Figure 6(c)) is caused by the fact that in a  $\pi$ -helix the translation per residue is 1.15 Å instead of 1.50 Å in a regular  $\alpha$ -helix. Figure 6(d) illustrates that even at high temperature the unfolding proceeds slowly and that the polyvalyl part comprising positions 15 to 21 retains an  $\alpha$ -helical fold during the 0.90 ns of simulation at 500 K. This is in strong contrast to the results from other high temperature simulations of peptides and proteins. For example, in the study of a 13-residue polyalanine by Daggett & Levitt (1992) the  $\alpha$ -helical conformation disappears within 10 ps at a temperature of 473 K and in a simulation of the thermal unfolding of hen egg white lysozyme, a globular protein of 129 residues consisting of both  $\alpha$ -helix and  $\beta$ -sheet, there is almost complete loss of secondary structure within 200 ps of simulation at 500 K (Mark & van Gunsteren, 1992). In fact it has been suggested that simulation force fields might be biased towards hastening polypeptide helix unfolding (Soman *et al.*, 1991).

Schreiber & Steinhauser (1992) have reported that the stability of an isolated  $\alpha$ -helix in aqueous simulations is an oscillating function of the length of the cutoff radius for electrostatic interactions. According to these authors a long-range cutoff of 1.4 nm, which was used in the present study, is actually strongly destabilizing and quickly (within 30 ps) leads to the unfolding of a 17-residue test peptide in water. To the contrary, SP-C in aqueous solution is stable, and it is also stable in methanol, the other medium where electrostatics by far dominate over the van der Waals contribution to the protein-solvent interaction energy (compare Table 5). The oscillating dependence of stability on the cutoff is, according to Schreiber & Steinhauser (1992), caused by the solute ordering the solvent molecules into concentric shells. Since the molecular radius of methanol is roughly one-fourth larger than that of water, the cutoff destabilization should be anticipated to be different in these two solvents. In the present study the stability of SP-C helix in water and methanol is similar. In chloroform, however, where the van der Waals' interactions strongly dominate

over the electrostatic contribution to the protein-solvent potential energy (Table 5), the extent of destabilization is greatest. It is unlikely that the arguments of Schreiber & Steinhauser (1992) in relation to the effect of cutoff on helix stability are relevant in the current study. The effects observed by Schreiber & Steinhauser (1992) may primarily be due to the fact that their study involved a 17-amino-acid-polypeptide chain with four evenly spaced charged residues. SP-C has only three positively charged residues (Arg2, Lys11 and Arg12) in the N-terminal part of the molecule, there are none in the main part of the  $\alpha$ -helix. Thus, the predominantly non-polar sequence of SP-C makes it relatively insensitive to the electrostatic cutoff.

The stability of the SP-C helix in the present simulations implies that there is a high activation energy barrier to any conformational transition. Whether the helical conformation corresponds to a metastable state or to the global free energy minimum, cannot be judged from the present data. Clearly, however, the shape of the free energy profile for conformational transitions is very much influenced by the solvent environment. One observation that supports the interpretation of there being a high activation energy barrier to a conformational transition from the helical state, is the fact that the native protein folds into an  $\alpha$ -helical conformation (Pastrana *et al.*, 1991; Vandebussche *et al.*, 1992; Johansson *et al.*, 1994b) while a synthetic peptide with the same sequence is less helical (Johansson *et al.*, 1995b). The signs of destabilization in the chloroform simulation indicate that the barrier to conformational transition is lowered in an apolar environment, apparently by favorable solvation of the aliphatic side-chains. Since the crossing of the same activation energy barrier is required for both folding and unfolding, it is likely that a predominantly hydrophobic (membrane) environment is required to facilitate the folding of SP-C.

The simulations indicate that the origin of this barrier is the stable and close packing of the valine side-chains which prevent competition of solvent molecules for backbone hydrogen bonding interactions. The unfolding starts from the C terminus. In the simulations at 300 K the hydrophobic middle part

of the helix is reasonably stable, and the polyvalyl segment in particular remains virtually intact. The low number of valine  $\chi^1$  transitions indicates restriction of side-chain rotation while the actual values of the  $\chi^1$  angles cluster around the most favorable rotamer of  $-65^\circ$ . This implies that the valine side-chains are locked into their positions, from which they unravel only successively upon unfolding. It has been shown in MD simulations that helix denaturation follows from the solvent molecules replacing the regular  $\alpha$ -helical hydrogen bonds (DiCapua *et al.*, 1991; Tirado-Rives & Jorgensen, 1991; De Loof *et al.*, 1992). In the SP-C simulations the bulky hydrophobic side-chains of valine, leucine and isoleucine residues effectively keep the solvent molecules away from approaching the backbone amide groups and competing for the  $\alpha$ -helical hydrogen bonds in polar media. A destabilizing solvent insertion into the SP-C  $\alpha$ -helix is observed mainly at the positions of Gly29 and Ala30.

Chloroform cannot replace the intramolecular hydrogen bonds. The break-up of the  $\alpha$ -helical hydrogen bonds in chloroform is caused by intramolecular interactions between the charged side-chains and the polar backbone groups. This is due in part to the poor solvation of the charged side-chains by the non-polar solvent. Such an effect can be assumed to be absent in the phospholipid bilayer environment of SP-C as the  $\alpha$ -helix spans the bilayer and the charged N-terminal residues interact with the dipalmitoyl-phosphatidylcholine head groups (Johansson *et al.*, 1995a). This should be taken into consideration when drawing parallels between the behaviour of the polypeptide in the chloroform simulation and its behavior in the biological environment. It should be emphasized again that though the greatest conformational flexibility was observed in chloroform, this does not mean that the helical conformation is not the thermodynamically most stable state in a hydrophobic solvent or in particular in a membrane environment. It only implies that the barriers to folding or unfolding are lower. In regard to the NMR-structure determination of SP-C in a mixed solvent of chloroform, methanol and 0.1M HCl in water (Johansson *et al.*, 1994b), the present MD-simulations show that the polar solvents play an important role for the conformational stability by solvating the charged side-chains and thereby preventing the polar intramolecular interactions.

The helix propensity of valine residues seems to be higher in the hydrophobic matrix of the SP-C than indicated by previous studies. As mentioned in the Introduction, experimental studies of oligopeptides where a valine probe residue was inserted in an alanine-based sequence indicated a low intrinsic preference for a helical conformation for valine residues (Merutka *et al.*, 1990; Padmanabhan *et al.*, 1990). The rationale for using an alanine-based matrix (Padmanabhan *et al.*, 1994) is to avoid side-chain interactions in order to obtain an intrinsic helix propagation parameter, an "s-value" (Zimm &

Bragg, 1959), which is independent of neighboring residues. Interactions between adjacent residues in turns, i.e. positions  $i + 3$  and  $i + 4$  from a residue  $i$ , are particularly important for helix stability. In the studies reported by Kallenbach and co-workers (Lyu *et al.*, 1990, 1991) where three guest residues were flanked by long polar side-chain residues, the destabilizing effect of valine residues was slightly lower. Valine residues appeared to be slightly helix-destabilizing also in the guest-host studies of Scheraga and co-workers (Wójcik *et al.*, 1990) where the guest residue was inserted into random copolymers containing hydroxypropylglutamine or hydroxybutylglutamine as host. In a theoretical treatment of helicity published by Finkelstein *et al.* (1991) hydrophobic interactions between non-polar side-chains are taken into account by estimating the size of hydrophobic surface screened in a close side-chain-side-chain contact and the fraction of rotamers that provide these contacts. The theory reproduces the s-value for valine from the guest-host studies (Wójcik *et al.*, 1990). A sequence consisting of non-polar branched residues as found in SP-C provides numerous helix-stabilizing side-chain interactions and buries effectively hydrophobic surface of an individual valine residue. In the present simulations the van der Waals contribution to the protein-protein potential energy dominates over the electrostatic contribution. The ratio between van der Waals and electrostatic contributions to the potential energy for the final conformation of the full-length protein were (in  $10^3$  kJ mol $^{-1}$ ):  $-0.84/-0.45$  in chloroform,  $-0.90/-0.10$  in methanol and  $-0.93/+0.29$  in water (the values are averages over the last 60 ps). This indicates that the cumulative effect of weak hydrophobic interactions is an important factor in stabilizing the  $\alpha$ -helix in SP-C. Similar observations have recently been made in other systems. For example, Matthews and co-workers (Blaber *et al.*, 1993, 1994) have done a mutational analysis at two solvent-exposed  $\alpha$ -helical sites in T4 lysozyme. Based on a clear correlation between the free energies of unfolding and the buried side-chain surface area they propose that the hydrophobic interaction most substantially contributes to helix stability.

## Summary

The simulations show that contrary to what might have been expected based on previously published values for the helix propensity of valine residues and previous simulation studies on the stability of soluble  $\alpha$ -helical peptides, the  $\alpha$ -helical fold of the valyl-rich, predominantly hydrophobic peptide SP-C is remarkably stable in water, methanol and to a lesser extent in chloroform. The simulations have been analyzed in regard to factors that have been previously proposed to affect the stability of valine-residue-containing  $\alpha$ -helices, that is, the main-chain and side-chain conformational entropy and possible strain, hydrogen-bonding network and solvent exposed surface. It has been shown that

backbone and side-chain dihedral angles do not deviate considerably from regular  $\alpha$ -helical geometry. The side-chain rotamer sampling of the valine residues is partially but not fully restricted. This implies some loss of configurational entropy upon helix formation. The stability of the helix is primarily attributed to the additive effect of van der Waals interactions due to the close packing of the branched aliphatic side-chains. This also prevents the solvent molecules from interacting with the protein backbone, especially in the polyvalyl part of Val15 to Val21. In the more polar solvents the interaction between the hydrophobic side-chains is enhanced leading to increased helix stability. In chloroform the unfolding process is slow, starting from the C-terminal end of the molecule and proceeding successively towards the N terminus. There is a contradiction between the C-terminal fraying and the NMR data in a mixed organic solvent. This discrepancy can, however, be attributed to the low pH in the experiments. Even at elevated temperature the polyvalyl stretch in the middle of the helical part of SP-C does not unfold. The results emphasize the stability of the  $\alpha$ -helical conformation of SP-C. They also demonstrate that the helix propensity of a given amino acid, in particular that of valine, can be highly sequence and environment specific. The apparent extreme stability of the valyl-rich  $\alpha$ -helix in SP-C also provokes the question whether consecutive valine residues are seldom found in  $\alpha$ -helices because they are intrinsically destabilizing or are selected against because of folding and unfolding considerations.

## Computational Methods

All simulations were performed using the GROMOS simulation package in conjunction with the GROMOS87 force field (van Gunsteren & Berendsen, 1987). Bond lengths were constrained to their standard values using the SHAKE algorithm (Ryckaert *et al.*, 1977) with a relative accuracy of  $10^{-4}$ , which allowed for a time step of 2 fs at 300 K. Non-polar hydrogen atoms were incorporated into the carbon atoms to which they are attached according to the united atom approach. Polar hydrogen atoms were treated explicitly. The N terminus as well Arg2, Lys11 and Arg12 were protonated. The C terminus was negatively charged. Non-bonded interactions were treated by the twin-range method (van Gunsteren & Berendsen, 1990). Within the short-range cutoff all interactions were determined every step, based on a pair list which was updated every 10 fs. Electrostatic interactions within the long-range cutoff were determined every 10 fs and held constant at intermediate steps. The appropriate temperature and the pressure of one bar were maintained by weak coupling to an external bath (Berendsen *et al.*, 1984) with coupling constants of 0.1 ps and 0.5 ps, respectively. Periodic boundary conditions were applied to avoid edge effects.

The initial set of atomic coordinates for the non-palmitoylated SP-C was generated using the molecular graphics package MIDAS (Ferrin *et al.*, 1988). The backbone angles of the residues Asn9 to Gly34 were set to canonical  $\alpha$ -helix values and the backbone angles of the remaining residues were set to  $180^\circ$ . The molecule was equilibrated *in vacuo* for 2 ns, whereafter a number of atom-atom distances was

restrained during 200 ps with 244 experimental NOE-based distance constraints (Johansson *et al.*, 1994b). Then again the molecule was subjected to free MD *in vacuo* for another 2 ns. The structure thus obtained fulfilled the NOE-constraints better than the original modeled structure (e.g. the number of violations  $>1.0 \text{ \AA}$  was 3 and 26, respectively). The N-terminal residues Cys6, Pro7 and Val8 which were initially modeled as extended chain, assumed an  $\alpha$ -helical conformation during this procedure. This structure was used as a starting structure in each of the three MD simulations of SP-C.

Details characterizing the simulations are presented in Table 5. The following solvent force fields were used: the simple point charge model (SPC) of Berendsen *et al.* (1981) for water, the model of Dietz & Heinzinger (1984, 1985) for chloroform, and the optimized model reported by Stouten (1989) for methanol as it accurately reproduced the experimental density of pure liquid methanol when applying the short and long-range cutoff values of 8  $\text{\AA}$  and 14  $\text{\AA}$ . The same electrostatic cutoffs were used in the water simulations, while in chloroform the value of both short and long-range cutoff was set to 1.4 nm. van der Waals  $C_6$  and  $C_{12}$  interaction parameters for interactions between protein and solvent atoms were obtained by taking the geometric mean of the self interaction parameters, i.e.  $C_6(i, j) = (C_6(i, i)C_6(j, j))^{1/2}$ . The combination rules for solvent-solvent interactions and solute-solute interactions were as defined in the original models and the GROMOS force field, respectively. For the interaction between a neutral carbon and SPC water oxygen a corrected value of  $C_{12}(OW,OW)^{1/2} = 793.3(\text{kcal mol}^{-1} \text{\AA}^{12})^{1/2}$  was used (Mark *et al.*, 1994). A truncated octahedron was chosen as a periodic box shape in order to allow for unhindered rotation of the solute. The box diameter was 80  $\text{\AA}$  between its quadratic edge planes in the chloroform and methanol simulations, and 74  $\text{\AA}$  in the water simulation. The minimum distance between the box wall and the maximum dimensions of the protein was in every case larger than 10  $\text{\AA}$ . Initially the solvent molecules with a protein-solvent distance (between non-hydrogen atoms) less than 2.3  $\text{\AA}$  in water, and 3.0  $\text{\AA}$  in chloroform and methanol were removed from the computational box. Each solution was equilibrated first by 130 steps of conjugate gradient energy minimization to remove gross van der Waals overlap between solute and solvent atoms. Initial velocities were taken from a Maxwell distribution at 300 K. Thereafter the system was further equilibrated by applying positional restraining for the protein during the first 5 ps of the simulation.

Simulation of SP-C in water is computationally significantly more expensive than simulations performed in either chloroform or methanol. This is due to both the total number of atoms (compare Table 5) and to the number of interaction pairs which fall within the short range cutoff. To enable an investigation of the stability of the helical region in SP-C in water for a longer time period at 300 K and to monitor the process of unfolding, two additional MD-simulations were performed on a truncated SP-C molecule lacking the five N-terminal residues. The initial atomic coordinates were generated using the molecular graphics package MIDAS (Ferrin *et al.*, 1988) while leaving out residues Leu1 to Cys5 and setting the backbone angles of residues Asn9 to Gly34 to  $\alpha$ -helical values. After energy-minimization the truncated SP-C molecule was simulated in water for 1 ns at 300 K in a rectangular box of size  $30 \times 31 \times 64 \text{ \AA}^3$ , and for 120 ps at 500 K in the same box. As the protein at the higher temperature rotated out of the box within a period of 120 ps, entailing a risk of interactions with its own periodic image, the simulation at

500 K was continued in a truncated octahedron with a diameter of 61 Å for an additional 780 ps. The high temperature run was done with a time step of 1 fs, updating the non-bonded pair list every 5 fs and without pressure coupling.

### Acknowledgement

H. K. acknowledges a grant from the Biotechnology Research Foundation in Sweden.

### References

- Baatz, J. E., Smyth, K. L., Whitsett, J. A., Baxter, C. & Absolom, D. R. (1992). Structure and functions of a dimeric form of surfactant protein SP-C: a Fourier transform infrared and surfactometry study. *Chem. Phys. Lipids*, **63**, 91–104.
- Berendsen, H. J. C., Postma, J. P. M., van Gunsteren, W. F. & Hermans, J. (1981). Interaction models for water in relation to protein hydration. In *Intermolecular Forces* (Pullman, B., ed.), pp. 331–342, Reidel, Dordrecht.
- Berendsen, H. J. C., Postma, J. P. M., van Gunsteren, W. F., Di Nola, A. & Haak, J. R. (1984). Molecular dynamics with coupling to an external bath. *J. Chem. Phys.* **81**, 3684–3690.
- Blaber, M., Zhang, X.-J. & Matthews, B. W. (1993). Structural basis of amino acid  $\alpha$ -helix propensity. *Science*, **260**, 1637–1640.
- Blaber, M., Zhang, X.-J., Lindstrom, J. D., Pepiot, S. D., Baase, W. A. & Matthews, B. W. (1994). Determination of  $\alpha$ -helix propensity within the context of a folded protein. *J. Mol. Biol.* **235**, 600–624.
- Chou, P. Y. & Fasman, G. D. (1978). Prediction of the secondary structure of proteins from their amino acid sequence. *Advan. Enzymol.* **47**, 45–148.
- Creamer, R. P. & Rose, G. D. (1992). Side-chain entropy opposes  $\alpha$ -helix formation but rationalizes experimentally determined helix-forming propensities. *Proc. Nat. Acad. Sci., U.S.A.* **89**, 5937–5941.
- Creighton, T. E. (1984). In *Proteins: Structures and Molecular Properties*, p. 171, W. H. Freeman and Co., New York.
- Curstedt, T., Johansson, J., Persson, P., Eklund, A., Robertson, B., Löwenadler, B. & Jörnvall, H. (1990). Hydrophobic surfactant-associated polypeptides: SP-C is a lipopeptide with two palmitoylated cysteine residues, whereas SP-B lacks covalently linked fatty acyl groups. *Proc. Nat. Acad. Sci., U.S.A.* **87**, 2985–2989.
- Daggett, V. & Levitt, M. (1992). Molecular dynamics simulations of helix denaturation. *J. Mol. Biol.* **223**, 1121–1138.
- De Loof, H., Nilsson, L. & Rigler, R. (1992). Molecular dynamics simulation of galanin in aqueous and non-aqueous solution. *J. Amer. Chem. Soc.* **114**, 4028–4035.
- DiCapua, F. M., Swaminathan, S. & Beveridge, D. L. (1991). Theoretical evidence for water insertion in  $\alpha$ -helix bending: molecular dynamics of Gly30 and Ala30 in vacuo and in solution. *J. Amer. Chem. Soc.* **113**, 6145–6155.
- Dietz, W. & Heinzinger, K. (1984). Structure of liquid chloroform. A comparison between computer simulation and neutron scattering results. *Ber. Bunsenges. Phys. Chem.* **88**, 543–546.
- Dietz, W. & Heinzinger, K. (1985). A molecular dynamics study of liquid chloroform. *Ber. Bunsenges. Phys. Chem.* **89**, 968–977.
- El Tayar, N., Mark, A. E., Vallat, P., Brunne, R. M., Testa, B. & van Gunsteren, W. F. (1993). Solvent-dependent conformation and hydrogen-bonding capacity of cyclosporin A: evidence from partition coefficients and molecular dynamics simulations. *J. Med. Chem.* **36**, 3757–3764.
- Ferrin, T. E., Huang, C. C., Jarvis, L. E. & Langridge, R. (1988). The MIDAS display system. *J. Mol. Graphics*, **6**, 13–27.
- Finkelstein, A. V., Badretdinov, A. Y. & Ptitsyn, O. B. (1991). Physical reasons for secondary structure stability:  $\alpha$ -helices in short peptides. *Proteins: Struct. Funct. Genet.* **10**, 287–299.
- Hartsough, D. S. & Merz, K. M., Jr (1993). Protein dynamics and solvation in aqueous and nonaqueous environments. *J. Amer. Chem. Soc.* **115**, 6529–6537.
- Hubbard, S. J. & Thornton, J. M. (1993). "Naccess", *Computer Program*, Department of Biochemistry and Molecular Biology, University College, London, U.K.
- Kabsch, W. & Sander, C. (1983). Dictionary of protein secondary structure: pattern recognition of hydrogen-bonded and geometrical features. *Biopolymers*, **22**, 2577–2637.
- Johansson, J., Curstedt, T., Robertson, B. & Jörnvall, H. (1988). Size and structure of the hydrophobic low molecular weight surfactant-associated polypeptide. *Biochemistry*, **27**, 3544–3547.
- Johansson, J., Curstedt, T. & Robertson, B. (1994a). The proteins of the surfactant system. *Eur. Respir. J.* **7**, 372–391.
- Johansson, J., Szyperski, T., Curstedt, T. & Wüthrich, K. (1994b). The NMR structure of the pulmonary surfactant-associated polypeptide SP-C in an apolar solvent contains a valyl-rich  $\alpha$ -helix. *Biochemistry*, **33**, 6015–6023.
- Johansson, J., Szyperski, T. & Wüthrich, K. (1995a). A structural basis for the function of the pulmonary surfactant-associated polypeptide SP-C. *FEBS Letters*, in the press.
- Johansson, J., Nilsson, G., Strömberg, R., Robertson, B., Jörnvall, H. & Curstedt, T. (1995b). Secondary structure and biophysical activity of synthetic analogs of the pulmonary surfactant polypeptide SP-C. *Biochem. J.* In the press.
- Lautz, J., Kessler, H., van Gunsteren, W. F., Weber, H.-P. & Wenger, R. M. (1990). On the dependence of molecular conformation on the type of solvent environment: a molecular dynamics study of cyclosporin A. *Biopolymers*, **29**, 1669–1687.
- Lide, D. R. (1993). *Handbook of Chemistry and Physics*, CRC Press, Boca Raton, Florida.
- Lyu, P. C., Liff, M. I., Marky, L. A. & Kallenbach, N. R. (1990). Side-chain contributions to the stability of alpha-helical structure in peptides. *Science*, **250**, 669–673.
- Lyu, P. C., Sherman, J. C., Chen, A. & Kallenbach, N. R. (1991).  $\alpha$ -Helix stabilization by natural and unnatural amino acids with alkyl side chains. *Proc. Nat. Acad. Sci., U.S.A.* **88**, 5317–5320.
- Mark, A. E. & van Gunsteren, W. F. (1992). Simulation of the thermal denaturation of hen egg white lysozyme: trapping the molten globule state. *Biochemistry*, **31**, 7745–7748.
- Mark, A. E., van Helden, S. P., Smith, P. E., Janssen, L. H. M. & van Gunsteren, W. F. (1994). Convergence properties of free energy calculations:  $\alpha$ -cyclodextrin complexes as a case study. *J. Amer. Chem. Soc.* **116**, 6293–6302.

- McGregor, M. J., Islam, S. A. & Sternberg, M. J. E. (1987). Analysis of the relationship between side-chain conformation and secondary structure in globular proteins. *J. Mol. Biol.* **198**, 295–310.
- Merutka, G., Lipton, W., Shalongo, W., Park, S.-H. & Stellwagen, E. (1990). Effect of central-residue replacements on the helical stability of a monomeric peptide. *Biochemistry*, **29**, 7511–7515.
- Mierke, D. F. & Kessler, H. (1991). Molecular dynamics with dimethyl sulfoxide as a solvent. Conformation of a cyclic hexapeptide. *J. Amer. Chem. Soc.* **113**, 9466–9470.
- Norin, M., Haefner, F., Hult, K. & Edholm, O. (1994). Molecular dynamics simulations of an enzyme surrounded by vacuum, water, or a hydrophobic solvent. *Biophys. J.* **67**, 548–559.
- O'Neil, K. T. & DeGrado, W. F. (1990). A thermodynamic scale for the helix-forming tendencies of the commonly occurring amino acids. *Science*, **250**, 646–651.
- Padmanabhan, S., Marqusee, S., Ridgeway, T., Laue, T. M. & Baldwin, R. L. (1990). Relative helix-forming tendencies of non-polar amino acids. *Nature (London)*, **344**, 268–270.
- Padmanabhan, S., York, E. J., Gera, L., Stewart, J. M. & Baldwin, R. L. (1994). Helix-forming tendencies of amino acids in short (hydroxybutyl-L-glutamine peptides: an evaluation of the contradictory results from host-guest studies and short alanine-based peptides. *Biochemistry*, **33**, 8604–8609.
- Pardi, A., Billeter, M. & Wüthrich, K. (1984). Calibration of the angular dependence of the amide proton-C $\gamma$  proton coupling constants,  $^3J_{\text{HN}\gamma}$ , in a globular protein. *J. Mol. Biol.* **180**, 741–751.
- Pastrana, B., Mautone, A. J. & Mendelsohn, R. (1991). Fourier transform infrared studies of secondary structure and orientation of pulmonary surfactant protein SP-C and its effect on the dynamic surface properties of phospholipids. *Biochemistry*, **30**, 10058–10064.
- Popot, J.-L. (1993). Integral membrane protein structure: transmembrane  $\alpha$ -helices as autonomous folding domains. *Curr. Opin. Struct. Biol.* **3**, 532–540.
- Robertson, B., Batenburg, J. J. & Golde, L. M. G. (1992). Editors of *Pulmonary Surfactant. From Molecular Biology to Clinical Practice*, Elsevier, Amsterdam.
- Ryckaert, J.-P., Ciccotti, G. & Berendsen, H. J. C. (1977). Numerical integration of cartesian equations of motion of a system with constraints: molecular dynamics of n-alkanes. *J. Comp. Phys.* **23**, 327–341.
- Schreiber, H. & Steinhauser, O. (1992). Cutoff size does strongly influence molecular dynamics results on solvated polypeptides. *Biochemistry*, **31**, 5856–5860.
- Shi, Y.-Y., Wang, L. & van Gunsteren, W. F. (1988). On the approximation of solvent effects on the conformation and dynamics of cyclosporin A by stochastic dynamics simulation techniques. *Mol. Simulat.* **1**, 369–383.
- Smythe, M. L., Huston, S. E. & Marshall, G. R. (1993). Free energy profile of a  $3_{10}$ - to  $\alpha$ -helical transition of an oligopeptide in various solvents. *J. Amer. Chem. Soc.* **115**, 11594–11595.
- Soman, K. V., Karimi, A. & Case, D. A. (1991). Unfolding of an  $\alpha$ -helix in water. *Biopolymers*, **31**, 1351–1361.
- Stouten, P. F. W. (1989). Small molecules in the liquid, solid and computational phases. Dissertation, University of Utrecht, The Netherlands.
- Tirado-Rives, J. & Jorgensen, W. L. (1991). Molecular dynamics simulations of the unfolding of an  $\alpha$ -helical analogue of ribonuclease A S-peptide in water. *Biochemistry*, **30**, 3864–3871.
- Tobias, D. J. & Brooks, C. L., III (1991). Thermodynamics and mechanism of  $\alpha$ -helix initiation in alanine and valine peptides. *Biochemistry*, **30**, 6059–6070.
- Tropp, J. (1980). Dipolar relaxation and nuclear Overhauser effects in nonrigid molecules: the effect of fluctuating internuclear distances. *J. Chem. Phys.* **72**, 6035–6043.
- van Buuren, A. R. & Berendsen, H. J. C. (1993). Molecular dynamics simulation of the stability of a 22-residue  $\alpha$ -helix in water and 30% trifluoroethanol. *Biopolymers*, **33**, 1159–1166.
- Vandenbussche, G., Clercx, A., Curstedt, T., Johansson, J., Jörnvall, H. & Ruyschaert, J.-M. (1992). Structure and orientation of the surfactant-associated protein C in a lipid bilayer. *Eur. J. Biochem.* **203**, 201–209.
- van Gunsteren, W. F. & Berendsen, H. J. C. (1987). *Groningen Molecular Simulation (GROMOS) Library Manual*, Biomos, Nijenborgh 4, 9747 AG Groningen, The Netherlands.
- van Gunsteren, W. F. & Berendsen, H. J. C. (1990). Computer simulation of molecular dynamics: methodology, applications and perspectives in chemistry. *Angew. Chem. Int. Ed. Engl.* **29**, 992–1023.
- van Gunsteren, W. F. & Karplus, M. (1982). Protein dynamics in solution and in a crystalline environment: a molecular dynamics study. *Biochemistry*, **21**, 2259–2274.
- Wójcik, J., Altmann, K.-H. & Scheraga, H. A. (1990). Helix-coil stability constants for the naturally occurring amino acids in water. XXIV. Half-cystine parameters from random poly(hydroxybutylglutamine-co-S-methylthio-L-cystein). *Biopolymers*, **30**, 121–134.
- Yun, R. H. & Hermans, J. (1991). Conformational equilibria of valine studies by dynamics simulation. *Protein Eng.* **4**, 761–766.
- Zimm, B. H. & Bragg, J. K. (1959). Theory of the phase transition between helix and random coil in polypeptide chains. *J. Chem. Phys.* **31**, 526–535.

Edited by R. Huber

(Received 13 October 1994; accepted 20 December 1994)